TISSUE ENGINEERING: Part A
Volume 21, Numbers 13 and 14, 2015

DOI: 10.1089/ten.tea.2014.0549

In Vitro Repair of Meniscal Radial Tear Using Aligned Electrospun Nanofibrous Scaffold

Kazunori Shimomura, MD, PhD,[1] Allison C. Bean, PhD,[1] Hang Lin, PhD,[1]
Norimasa Nakamura, MD, PhD,[2,3] and Rocky S. Tuan, PhD[1]

Radial tears of the meniscus represent one of the most common injuries of the knee, and result in loss of biomechanical meniscal function. However, there have been no established, effective treatments for radial meniscal tears. Nanofibrous materials produced by electrospinning have shown high promise in the engineering of soft musculoskeletal tissues. The goal of our study is to apply these technologies to develop a functional cell-seeded scaffold as a potential, new surgical method to enhance meniscal radial repair. Cylinder-shaped explants were excised from the inner avascular region of bovine meniscus and a radial tear was created in the center of the explant. The torn site was wrapped with either nanofibrous scaffold alone or scaffold seeded with meniscal fibrochondrocytes (MFC). A control group was prepared as explants without scaffolds or cells. The composite constructs in each group were cultured *in vitro* for 4 and 8 weeks, and these were then assessed histologically and mechanically. Histological analysis showed partial repair of the radial tear was observed with adherence between scaffold and native meniscal tissue in either the scaffold alone or cell-seeded scaffold group. Only the cell-seeded scaffold exhibited significant positive Picrosirius red staining and Safranin O staining. Mechanical testing of the repaired meniscus showed that the load-to-failure and stiffness values were significantly improved in the cell-seeded group. These results demonstrated the applicability of the MFC-seeded nanofibrous scaffold for meniscal radial tear repair based on both histological and mechanical analyses. In particular, the highly adhesive property of the cell-seeded scaffold to the meniscal tissue should be beneficial in helping to preserve the meniscal function by stabilizing meniscal fibers.

Introduction

The meniscus plays important roles in the knee joint, including force transmission, shock absorption, and provision of joint stability.[1–5] Importantly, meniscal tears are the most common injury of the knee regardless of age, and loss of the meniscus is recognized to predispose the knee joint to degenerative changes, inevitably leading to osteoarthritis, as the meniscus has limited healing potential owing to limited blood supply.[6–8] An additional anatomical feature of meniscus is that it has a highly specialized arrangement of collagen fibers,[9,10] with the majority being circumferentially aligned. This circumferential orientation creates biomechanically optimal resistance to hoop stresses, resulting from displacement of the meniscus from the tibial plateau during normal weight-bearing.[11] Therefore, radial tears of the meniscus, which separate the circumferential meniscal fibers, cause loss of biomechanical meniscal function.[12] Clinically, radial tears have been mostly treated by partial meniscectomy, because this type of meniscal tear includes lesion of the avascular inner part of the meniscus and spontaneous healing is not expected.[13] To overcome these potential problems and preserve important meniscal functions, meniscal repair is being considered as an alternative treatment for radial tears that involve avascular lesion, and several suture techniques have been developed in recent meniscal radial tear surgical repairs. van Trommel *et al.* repaired five radial tears of the lateral meniscus using outside-in sutures enhanced by fibrin clot.[14] Noyes and Barber-Westin reported four cases of radial tear repairs using inside-out sutures.[15] Tao and Beach used a Caspari suture punch to repair one radial tear of the lateral meniscus.[16] Choi *et al.* reported 14 cases of radial tears of the midbody of the lateral meniscus with all-inside meniscal repair.[12] However, the number of patients treated with these suture techniques was small and limited in these reported studies. Moreover, the rate of complete healing has been low, and satisfactory clinical results have not been obtained.

[1]Center for Cellular and Molecular Engineering, Department of Orthopaedic Surgery, University of Pittsburgh School of Medicine, Pittsburgh, Pennsylvania.
[2]Institute for Medical Science in Sports, Osaka Health Science University, Osaka, Japan.
[3]Center for Advanced Medical Engineering and Informatics, Osaka University, Suita, Osaka, Japan.

Tissue engineering approaches that involve the use of biomaterial scaffolds have gained increasing attention as potential regenerative therapies in a number of disciplines, including musculoskeletal medicine. Among the biomaterial scaffolds, electrospun fibers have received attention because they can mimic both the structural and mechanical anisotropy of fibrous tissues and potentially withstand the mechanical loads imposed on the tissues during normal physiological motion.[17] In our previous studies, we have observed that adult mesenchymal stem cells (MSCs) cultured on aligned poly(ε-caprolactone) (PCL) nanofiber scaffolds fabricated by electrospinning organize and deposit collagen along the fiber direction, producing cartilage-like engineered constructs.[18,19] On the other hand, one drawback of electrospun materials is that the structure is quite dense, which can limit cell infiltration into the scaffold.[20] Also, this feature may influence the adhesive property to native tissue. To promote cell infiltration, Ionescu and Mauck[21] modified the porosity of PCL scaffold by incorporating water-soluble polyethylene oxide (PEO) as sacrificial fibers by using multi-jet electrospinning, and demonstrated that the highly porous scaffold improved the integration property between scaffold and native meniscus and cell infiltration into scaffold without the loss of mechanical property. Therefore, wrapping the radial tear with the cell-seeded modified PCL scaffold could be a potential, clinically relevant approach, as it would be mechanically stronger than suture alone,[22] by mechanically stabilizing the torn site and promoting the meniscal repair mediated by cells seeded within the scaffold.

To date, there have not been any studies that focus on the repair of meniscal radial tear using an *in vitro* model, although there were several *in vitro* models of meniscal repair with the use of meniscal explant from the avascular zone of meniscus.[23–25] Also, these studies have employed a defect model,[26] sandwich model,[23] and ring-shape (cylinder) model,[21,27,28] which did not take into account the circumferential fiber arrangement in the meniscus. Therefore, there is a need for an *in vitro* model to evaluate meniscal repair in terms of radial tear.

In this study, our goal is to produce a cell-seeded scaffold for meniscal repair for potential regenerative surgery application to enhance meniscal radial repair, and to demonstrate its feasibility with a newly developed *in vitro* model of meniscal repair.

Materials and Methods

Cell isolation

Meniscal explants were harvested from the hind-leg stifle of 2- to 3-year-old bovine within 24 h of slaughter (JW Treuth and Sons, Baltimore, MD). Meniscal fibrochondrocytes (MFCs) were aseptically isolated from the inner avascular part of the meniscus by first mincing the tissue into small pieces and then allowing cells to migrate out onto tissue culture plates to establish primary cultures according to the method reported by Mauck colleagues[21,29,30] For expansion, cells were cultured in growth medium consisting of DMEM-high glucose (Gibco, Carlsbad, CA), 10% v/v fetal bovine serum (FBS; Gibco), and 100 units/mL penicillin and 100 μg/mL streptomycin (Gibco). At 80% confluence, cells were detached with 0.25% w/v trypsin in 1 mM EDTA (Gibco) and passaged. All experiments were performed with passage 3 bovine MFCs.

Fabrication of aligned electrospun scaffold

To create electrospun scaffolds, two separate solutions of (1) 11.5% w/v PCL (80 kDa; Sigma-Aldrich, St. Louis, MO) in a 1:1 mixture of tetrahydrofuran (THF; Fisher Chemical, Fairlawn, NJ) and N,N-dimethylformamide (DMF; Fisher Chemical) including 0.06% NaCl, and (2) 10% PEO (200 kDa; Polysciences, Warrington, PA) in 90% ethanol were prepared by mixing overnight before electrospinning. To fabricate aligned scaffolds, a custom-designed electrospinning device was utilized to generate a 40:60 composite scaffold consisting of PCL and PEO fibers. Two 20-mL syringes were separately filled with the PCL and PEO electrospinning solution, and they were fitted with a stainless steel 22 G blunt-ended needle that served as a charged spinneret, and directed at a single central rotating mandrel (surface velocity of 10 m/s). The speed of the mandrel was sufficiently fast to align the collected fibers in a single direction. A flow rate of 2 mL/h was maintained with a syringe pump (Harvard Apparatus, Holliston, MA). A power supply (Gamma High Voltage Research, Inc., Ormond Beach, FL) applied a +15–20 kV potential difference between the needles and grounded mandrel to acquire a stable Taylor cone. Additionally, two aluminum shields charged to +10 kV were placed perpendicular to and on either side of the mandrel to better direct the electrospun fibers toward the grounded mandrel. The distance between the mandrel and the needle was 15 cm for PCL fibers and 10 cm for PEO fibers. The composite electrospun mat consisting of PCL and PEO fibers was generated with a final thickness of 500 μm. Scaffolds were imaged by scanning electron microscopy (SEM, field emission, JSM6335F; JEOL, Peabody, MA) after PEO removal (see below) to examine the alignment and diameter of PCL fibers. Ten PCL fibers were randomly selected from the SEM images, and a mean diameter of the fibers was calculated by Image J (National Institutes of Health, Bethesda, MD).

Production of cell-seeded scaffold

Each scaffold was cut into a rectangular shape (5 × 8 mm) of ~500 μm in thickness, sterilized by immersion in 70% ethanol for 2 h, and then washed in phosphate-buffered saline (PBS) twice, 30 min for each wash. PEO was removed from the scaffold by immersion in PBS for 12 h. Passage 3 MFCs were seeded at a density of 100,000 cells/scaffold onto the surface of prewetted scaffolds. After 1 h incubation at 37°C, additional 100,000 cells/scaffold were seeded on the reverse side of the scaffold in the same manner. After 1 h incubation at 37°C, scaffolds were incubated in growth medium at 37°C for 24 h to allow MFCs to diffuse into and adhere to the scaffold. After 24 h, the MFC-seeded scaffold was used for subsequent experiments. Also, cell adhesion and migration into the scaffold were estimated by DAPI nuclear staining.

Formation of composite constructs of meniscus and scaffold

Adult bovine menisci were aseptically harvested in the same manner mentioned above, and cylinder-shaped explants (5 mm diameter × 10 mm height) were then excised from the inner avascular region using a sterile disposable

biopsy punch (5 mm; Integra Miltex, York, PA) (Fig. 1A–C). Two to three explants were harvested from one meniscus, with the long axis aligned along the direction of the meniscal circumferential main fibers (Fig. 1A). A tear of half depth was created in the center of the explant, and radial tear was mimicked by cutting perpendicular to the meniscal main fibers (Fig. 1D). The torn site was wrapped with either the scaffold alone or MFC-seeded scaffold (scaffold group and cell group, respectively), with the scaffold fiber direction matching that of the meniscal main fibers. The scaffold was fixed to the meniscal explant with sutures to prevent detachment from its surface. A control group was prepared as explants without scaffolds or cells. The composite constructs in each group were cultured with growth medium consisting of DMEM-high glucose, 10% FBS, 100 units/mL penicillin and 100 μg/mL streptomycin, 50 μg/mL ascorbic acid 2-phosphate, and 10 ng/mL TGF-β3 (PeproTech, Rocky Hill, NJ) for 4 and 8 weeks, and these were then assessed by histology and mechanical testing.

Cell viability

At 1, 4 and 8 weeks postculture, the meniscus/scaffold constructs ($n=2$ per group) were washed twice with PBS and cell viability was assessed with the Live/Dead stain (Invitrogen, San Diego, CA) as examined by epifluorescence microscopy (live cells stained green, dead cells stained red). Three different slices of the samples from each group were prepared, and the number of live and dead cells was counted to calculate cell viability, represented as the percentage of number of live cells as a function of total number of live and dead cells.

Histology and immunohistochemistry

The constructs at 4 and 8 weeks postculture ($n=2$ per group) were washed twice in PBS, fixed in 4% paraformaldehyde for 2 h at 4°C, immersed in 30% sucrose solution for 12 h at 4°C, and then embedded in Tissue-Tek OCT compound (Sakura Finetek USA, Inc., Torrance, CA). Constructs collected before culture were prepared in each group as time zero (preculture) control. The embedded samples were sectioned at 8 μm thickness and stained with Picrosirius red for collagen, Safranin O/Fast green for sulfated glycosaminoglycans (GAGs), and DAPI to identify cell nuclei. The repair of radial tear was evaluated in the following manner to obtain an ''adhesion index.'' Three different sections of the gap area of the tissue stained with Picrosirius red were prepared in each group, and then the entire length of the cut edge in the radial tear and the length of adhesion site were outlined and measured by Image J (National Institutes of Health). The adhesion index was determined as the length of the adhesion site represented as a percentage of the total length of the cut edge.

The presence and distribution of collagen types I and II, and aggrecan were evaluated for the torn site at 8 weeks postculture using standard fluorescence immunohistochemistry. Briefly, sections were fixed in 4% paraformaldehyde for 5 min, treated with 0.1% Triton X-100 for permeabilization of cell membranes for 15 min, blocked with 1% bovine serum albumin for 1 h, and incubated with specific primary antibodies for 2 h at room temperature, followed by incubation with secondary antibodies for 1 h. The primary antibodies included mouse monoclonal anti-collagen type I

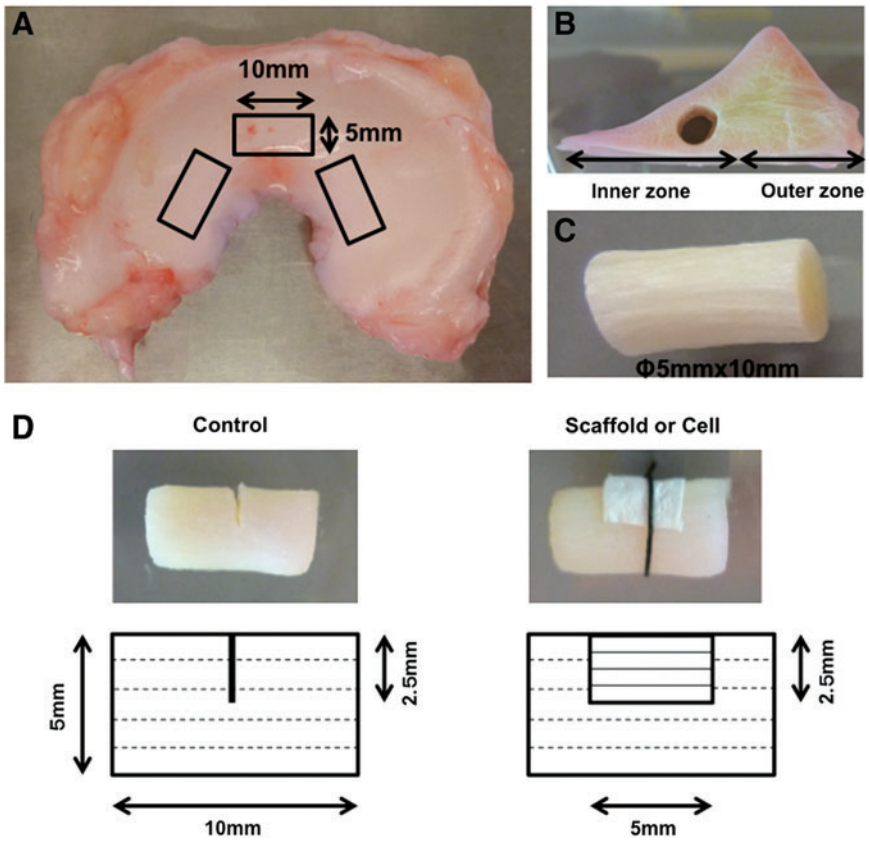

FIG. 1. Preparation of composite constructs of meniscus and scaffold. **(A–C)** Cylinder-shaped explants (5 mm diameter × 10 mm height) were excised from the inner avascular region of the meniscus, with the long axis aligned along the direction of the meniscal circumferential fibers. **(D)** Schematic illustration of the *in vitro* model of meniscal repair for radial tear in each group. *Dotted line* in the meniscal construct represents meniscal fiber direction and *solid line* in the scaffold represents scaffold fiber direction. Scaffold, scaffold only; cell, cell-seeded scaffold. Color images available online at www.liebertpub.com/tea

antibody (1:250, ab23446; Abcam, Cambridge, MA), mouse monoclonal anti-collagen type II (1:250, ab3092-500; Abcam), and mouse monoclonal anti-aggrecan antibody (1:250, ab3773-1; Abcam), with Alexa 488-labeled polyclonal goat anti-mouse IgG antibodies (1:2000; Molecular Probes, Eugene, OR) used as secondary antibodies. Negative controls for collagen type I or aggrecan were incubated without the use of the primary antibody. Positive control for collagen type II was prepared with histological sections of native inner meniscus.

Mechanical testing

Mechanical testing was performed using a Bose 3230 Mechanical Tester (Eden Prairie, MN) consisting of a 225 N load cell. At 4 and 8 weeks postculture, constructs ($n = 5$–7 per group) were washed twice in PBS, and a semicylindrical explant containing the repair site was harvested by precisely cutting with a plastic cutting guide. The explant was fixed to the mechanical tester at both ends of the construct. A similar, semicylindrical explant (5 mm diameter $\times$ 10 mm height) was also harvested from the preculture construct. The samples were preloaded to remove slack and then subjected to 5 mm strain at an elongation rate of 0.0833 mm/s to obtain load/displacement curve. For each construct, load to failure, stiffness, and Young's modulus of the repaired site were calculated.

Statistical analysis

Statistical analysis was performed using analysis of variance followed by *post hoc* testing for cell viability, adhesion index, and mechanical testing. The results are presented as mean $\pm$ SD. The data were analyzed with SPSS 21.0 (IBM SPSS, Chicago, IL) and significance was set at $p < 0.05$.

Results

Scaffold architecture and cell distribution in scaffold

SEM analysis revealed that highly aligned PCL fibers were obtained with a mean diameter of 471 $\pm$ 133 nm (Fig. 2A). DAPI staining demonstrated that seeded cells successfully migrated into the scaffold with most of them localized to the surface area of the scaffold (Fig. 2B, C).

Cell viability analysis

At 1 week postculture, a high percentage of viable cells was detected by Live/Dead assay in each group (control, 82.8% $\pm$ 4.4%; scaffold only, 85.7% $\pm$ 5.8%; and scaffold with cells, 86.7% $\pm$ 0.6%) (Fig. 3A, B). At 4 weeks, the majority of cells remained viable in each group (control, 86.4% $\pm$ 2.8%; scaffold only, 82.4% $\pm$ 6.4%; and scaffold with cells, 83.0% $\pm$ 4.1%). Even after 8 weeks of culture, cells maintained a high level of viability in each group (control, 83.9% $\pm$ 4.0%; scaffold only, 84.2% $\pm$ 8.8%; and scaffold with cells, 83.6% $\pm$ 10.6%), consistent with histological and mechanical testing observations (see below).

Histological analysis

DAPI staining showed that cells were recruited into the gap of radial tear in each group at 4 and 8 weeks (Fig. 4A). Matrix staining with Picrosirius red showed that the radial tear wrapped with the scaffold alone or cell-seeded scaffold exhibited partial repair at 4 weeks (adhesion index: 43.8% $\pm$ 22.9% and 59.5% $\pm$ 4.5%, respectively). However, complete repair was not observed in either group even after 8 weeks in culture, although the cell-seeded group showed overall improved healing compared to the scaffold only group (adhesion index: 83.0% $\pm$ 4.0% vs. 55.2% $\pm$ 21.5%, $p = 0.0083$) (Fig. 4B, C), and the control group showed a persistent gap even after 8

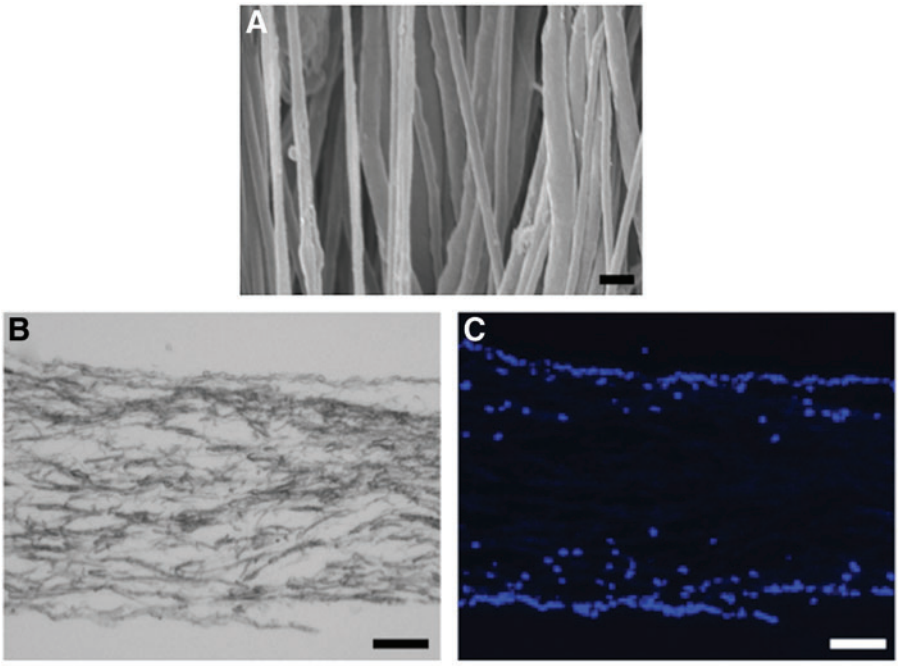

FIG. 2. Scaffold architecture and distribution of cells seeded in scaffold. **(A)** Scanning electron microscopy (SEM) showed that highly aligned poly(ε-caprolactone) (PCL) fibers were obtained. Scale bar = 1 μm. **(B)** Bright field image and **(C)** DAPI staining (*blue*, cell nuclei). Seeded cells were observed to have migrated into the scaffold. Scale bar = 100 μm. Color images available online at www.liebertpub.com/tea

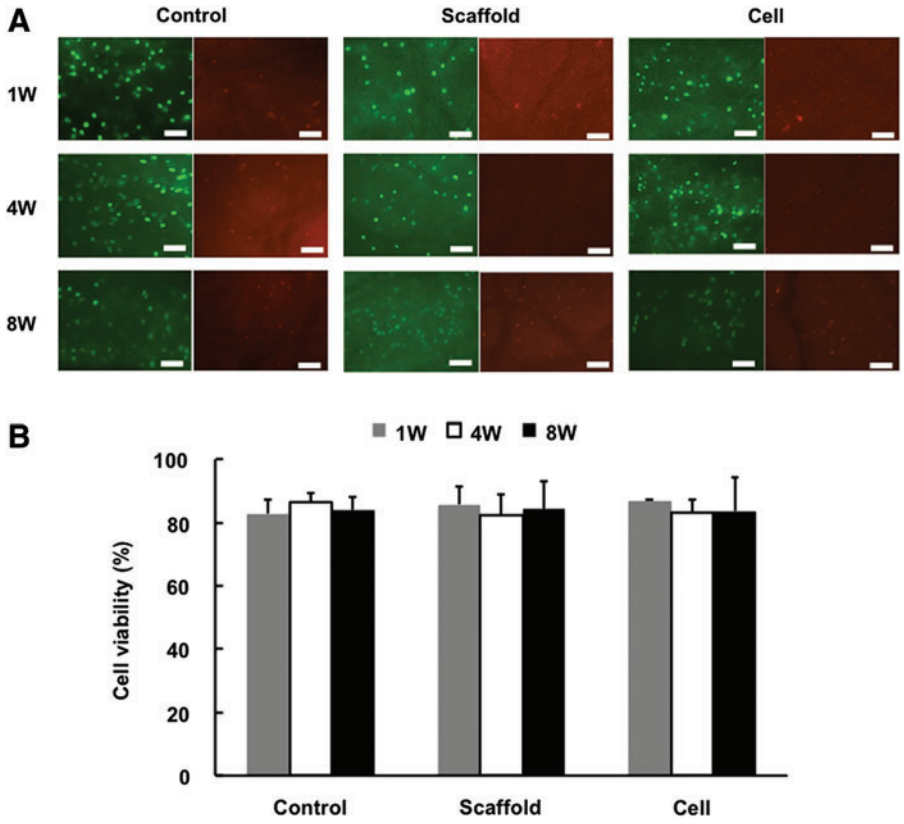

FIG. 3. Cell viability analysis. **(A)** Live/dead cell viability staining (*green*, live cells; *red*, dead cells) showed a high percentage of viable cells in each group at 8 weeks postculture. Scale bar = 100 μm. **(B)** Cell viability was more than 80% in each group. Color images available online at www.liebertpub.com/tea

weeks in culture. Immunohistochemical analysis of the torn site showed strong staining for collagen type I at the surface area of the radial tear in each group (Fig. 5). Aggrecan was detected at a low level in the same area in each group. On the other hand, collagen type II was not detected in any group.

DAPI staining showed evidence of cell migration into the center of the scaffold in each group at 4 and 8 weeks, and even, diffuse cell distribution was seen over the entire scaffold (Fig. 6A). The nanofibrous biomaterial scaffold, irrespective of cell-seeding, was observed to closely adhere to the native meniscal tissue at 4 and 8 weeks (Fig. 6B, C). Notably, the cell-seeded scaffold closely adhered to the native meniscal tissue without any gap in the preculture control. Also, the surface of the scaffold exhibited positive Picrosirius red staining in both the scaffold only and cell-seeded groups, while the scaffold inside also showed similar, uniform, weak Picrosirius red staining in both group (Fig. 6B). In contrast, only the cell-seeded group showed positive Safranin O staining (Fig. 6C).

Mechanical properties

Mechanical testing of the repaired meniscus explants showed that the load-to-failure (Fig. 7A) and stiffness values (Fig. 7B) in the cell-seeded group at 8 weeks were significantly higher than the control group at 4 (42.1 ± 18.7 vs. 3.3 ± 8.3 N, $p = 0.0074$; and 27.3 ± 15.8 vs. 2.3 ± 5.0 N/mm, $p = 0.0040$, respectively) and 8 weeks (42.1 ± 18.7 vs. 6.1 ± 14.9 N, $p = 0.0156$ and 27.3 ± 15.8 vs. 2.5 ± 4.9 N/mm, $p = 0.0044$, respectively). The Young's modulus in the cell-seeded group at 8 weeks was significantly higher than that of control group at 4 weeks (12.4 ± 8.6 vs. 0.85 ± 2.0 N/mm^2, $p = 0.0355$) (Fig. 7C). Also, it is noteworthy that the value of these parameters of the cell group at 8 weeks was ~40% of those of a normal meniscus (Fig. 7A–C).

Discussion

Radial tears of the menisci represent a common orthopedic injury, as Magee *et al.* reported a 14% incidence of radial tears among 200 patients who underwent arthroscopy.[31] Partial meniscectomy to remove the damaged, unstable portion of the meniscus has been the gold standard of surgical treatment for radial meniscal tears, while several long-term clinical studies showed a high risk of progression of knee osteoarthritis after meniscectomy.[1] It is thus important to preserve meniscal tissue in the knee, necessitating the development of an effective surgical technique of meniscal repair. In this *in vitro* study, we have demonstrated the feasibility of the MFC-seeded scaffold to repair the meniscal radial tear based on both histological and mechanical analyses. Therefore, this novel method of wrapping the radial tear with the scaffold should be further evaluated using *in vivo* models to assess its potential as a new surgical method with high clinical relevance (Fig. 8). Also, this technique may be useful for other currently untreatable meniscal tears, including multiple tears, similar to the Henning method of fascia sheath coverage for these tears combined with fibrin clot.[22]

Notably, the aligned nanofibrous scaffold was highly adhesive to the native meniscal tissue, and with cell-seeding, repair of the radial tear was improved, accompanied by observable increase in major extracellular matrix components of the meniscus, that is, collagen type I and aggrecan,

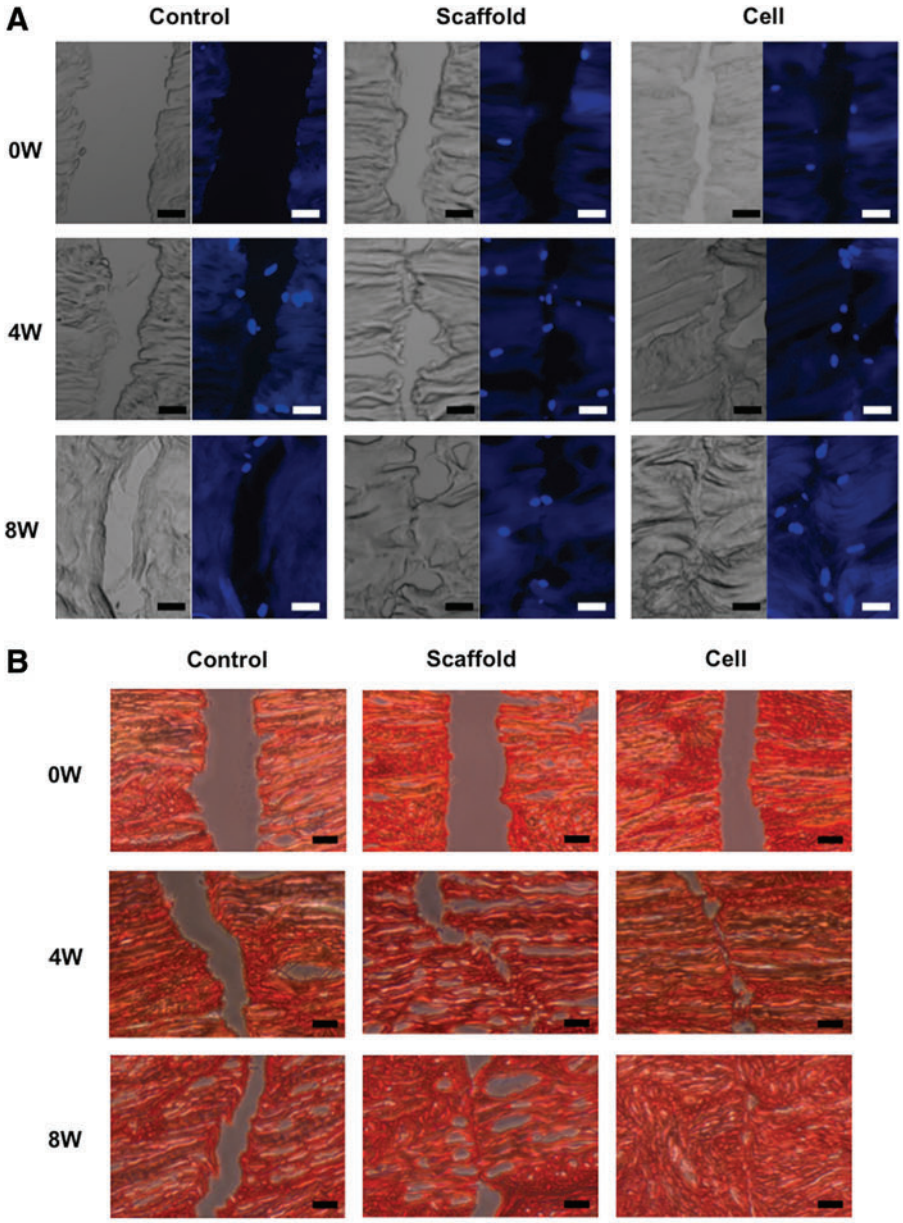

FIG. 4. The gap of radial tear in each group analyzed histologically by DAPI and Picrosirius red staining, and immunohistochemistry. **(A)** DAPI staining showed that in each group, cells were recruited into the gap of radial tear after 4 weeks of culture. Scale bar = 100 μm. **(B)** Picrosirius red staining showed that the radial tear wrapped with the scaffold alone or cell-seeded scaffold exhibited a partial repair, while the gap in the control group remained even after 8 weeks in culture. Scale bar = 100 μm. **(C)** The cell-seeded group showed overall improved healing compared to the scaffold group at 8 weeks, as analyzed based on the adhesion index. $*p < 0.05$; $**p < 0.01$. Color images available online at www.liebertpub.com/tea

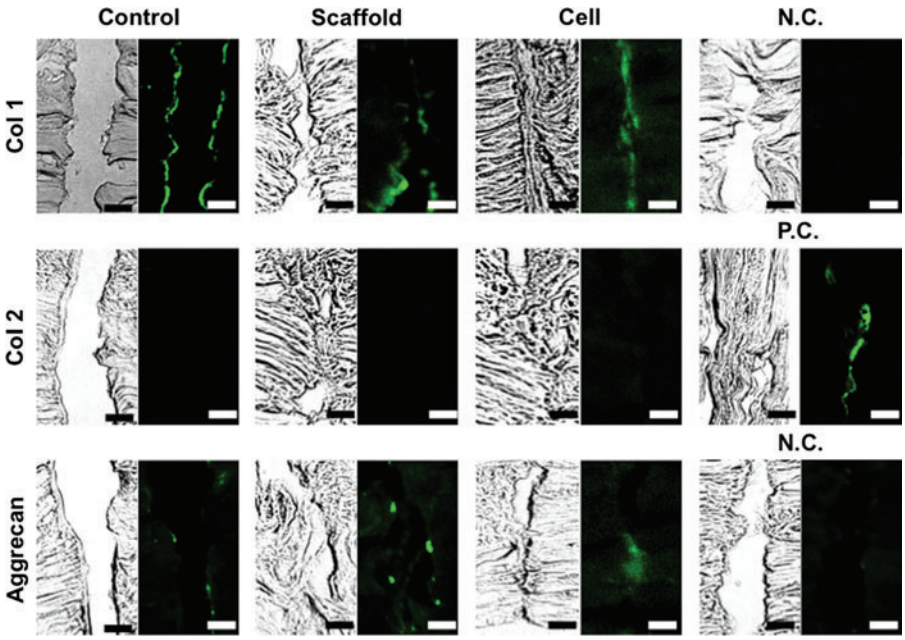

FIG. 5. Immunohistochemical analysis showed strong collagen type I staining and weak but detectable aggrecan staining and absent collagen type II present at the surface area of the radial tear in each group. Scale bar = 100 μm. Color images available online at www.liebertpub.com/tea

in the torn site, which was considered to promote the fibrocartilagenous repair process.[32] In comparison, in the control group without the scaffold wrap, the torn site was observed to remain as a gap until 8 weeks postculture, and it is thus mechanically unstable due to the lesion. Therefore, this adhesive property of the nanofibrous scaffold should also be considered as beneficial to stabilization of the meniscal circumferential fibers, thus contributing to the functional preservation of the hoop structure and perhaps preventing the development of osteoarthritis.

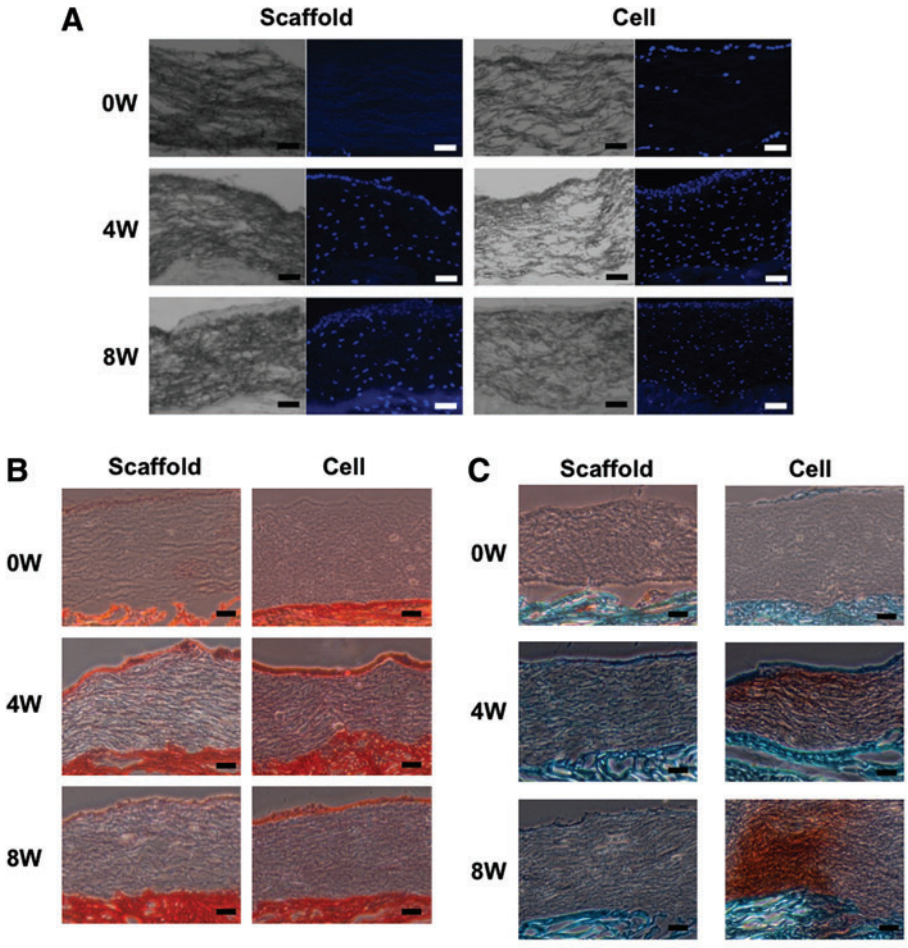

FIG. 6. Histological analysis of scaffold and adjacent meniscal tissue with DAPI, Picrosirius red, and Safranin O/Fast green staining. **(A)** DAPI staining showed that cells appeared to have migrated into the center of scaffold in each group at 4 and 8 weeks. **(B, C)** The scaffold, irrespective of cell-seeding, was observed to closely adhere to the native meniscal tissue at 4 and 8 weeks. Also, the scaffold exhibited positive Picrosirius red staining in both the scaffold only and cell-seeded scaffold groups, while only the latter showed positive Safranin O staining. Scale bar = 100 μm. Color images available online at www.liebertpub.com/tea

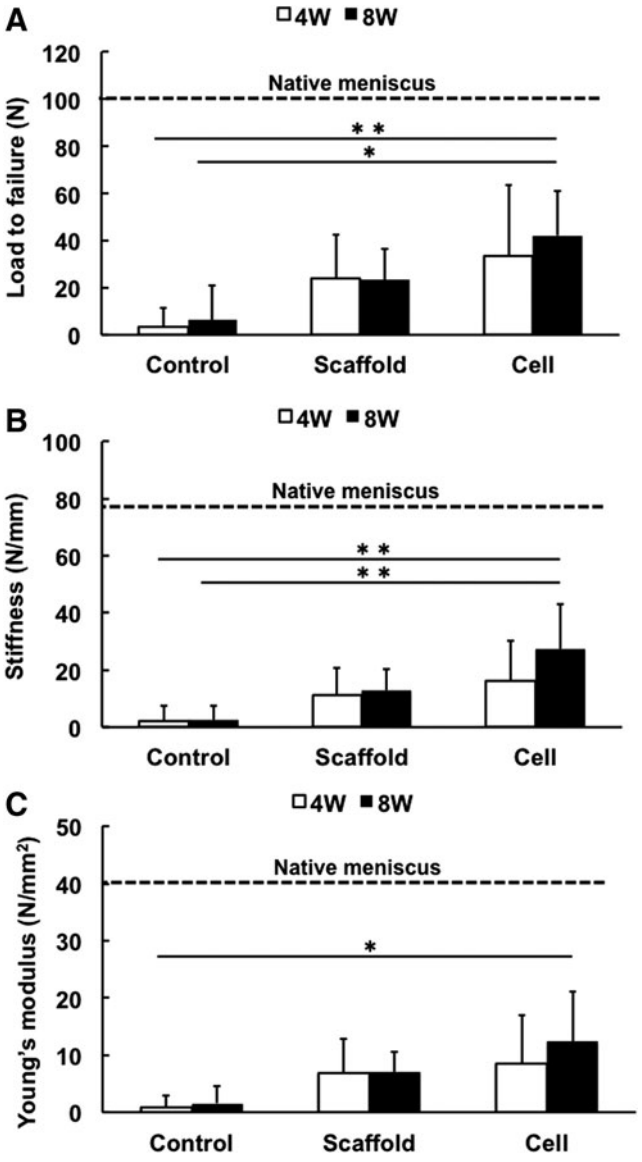

FIG. 7. Mechanical testing of repaired meniscus at 4 or 8 weeks of culture. The load-to-failure **(A)** and stiffness values **(B)** in the cell-seeded scaffold group at 8 weeks were significantly higher than those of the control group at 4 and 8 weeks. **(C)** Young's modulus value of the cell-seeded scaffold group at 8 weeks was significantly higher than that of the control group at 4 weeks. $*p<0.05$; $**p<0.01$.

Morphologically, the aligned nanofibrous scaffold has the structural anisotropy of fiber arrangement similar to that of meniscal collagen fibers,[18,19] and may work as ''a bridge'' to prevent widening of the gap at the torn site until the lesion is completely healed. In addition, the scaffold allowed successful cell infiltration and the deposition of a fibrocartilaginous matrix containing collagen and proteoglycan. Therefore, the cell-seeded nanofibrous scaffold could be expected to not only repair radial tears but also allow tissue remodeling to give rise to native meniscus-like tissue.

The physical and biological characteristics of the cell-seeded electrospun PCL scaffold appear to be superior to those seen with other biomaterial scaffold.[18,33] However, its mechanical properties are still lower than those of the native meniscus[20,34–36]; the mechanical testing results here showed that the repair tissue with MFC-seeded scaffold exhibited $\sim 40\%$ restoration compared to native meniscus. It should be noted that in the *in vitro* model these mechanical properties resulted from the combination of the integration of torn site and the adhesiveness between scaffold and native tissue, while in clinical practice the scaffold wrapping for radial tear would be combined with additional suture for better mechanical stabilization of the torn site. In addition, under *in vivo* condition, synovial fluid and other surrounding tissues, including cartilage and synovium, may also enhance repair in the meniscal lesion. Therefore, the application of this technique in clinical practice is likely to contribute both mechanically and biologically to meniscal repair.

Our results also show that the *in vitro* model described here would be useful for evaluating the reparative efficacy of candidate-engineered constructs or therapeutics, such as growth factors and pharmacological agents before *in vivo* testing. Accordingly, the use of the *in vitro* model described here may contribute toward both the analysis of the underlying mechanisms and the efficacy of potential therapeutic methods of meniscal repair.

While MSCs have been employed in many of the cell-based meniscal repair studies,[37,38] meniscus-derived cells could be a good cell source because these cells showed strong proliferative and fibrocartilaginous differentiation capacities, as reported in previous studies.[29,30] Also, regarding the method of cell isolation, we isolated MFCs from small pieces of meniscal tissue without collagenase, using a previously published method.[21,29,30] While collagenase is commonly used in cell isolation, given that collagenase preparations contain animal- or bacteria-derived components and may result in complications related to immune

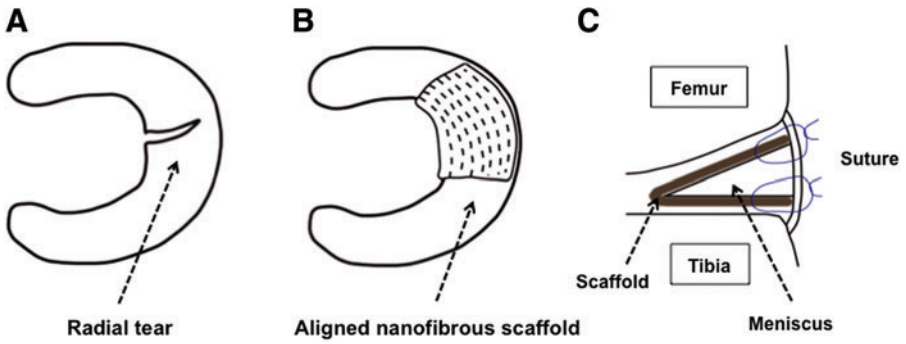

FIG. 8. Schematic representation of potential clinical application of the scaffold wrapping technique for the repair of meniscal tear. **(A)** Typical meniscal radial tear, **(B)** scaffold wrapping applied for radial tear with the scaffold fiber orientation matching that of meniscal main fibers, and **(C)** scaffold fixation with additional sutures for joint capsule. Color images available online at www.liebertpub.com/tea

reaction and cytotoxity,[39,40] we have chosen to use a safer, collagenase-free cell isolation method.

An obvious limitation of the present study is that *in vitro* culture is fundamentally different from the intra-articular environment, which includes the presence of synovium, cartilage, ligaments, and blood vessels, in addition to load-bearing and physical and mechanical changes. Nevertheless, we believe that the *in vitro* model presented here may serve as an initial proof-of-concept platform that will contribute toward experimental design of subsequent animal studies.

Conclusions

Our results showed that an MFC-seeded nanofibrous scaffold wrapped onto a meniscal radial tear enhanced the repair of the meniscus by strengthening the interface of the torn site, recruiting cells, and promoting their differentiation into fibrocartilaginous tissue. Also, these scaffolds contributed to increased mechanical strength at the site of the meniscal tear. Upon further development, we believe this approach may be applied in clinical practice to repair current surgically untreatable meniscal tears to minimize the development of osteoarthritis.

Acknowledgment

This project is supported by grants from Commonwealth of Pennsylvania Department of Health (SAP-4100050913), USA, and Osaka Sports Medicine Association, Japan.

Disclosure Statement

No competing financial interests exist.

References

1. McDermott, I.D., and Amis, A.A. The consequences of meniscectomy. J Bone Joint Surg Br **88,** 1549, 2006.
2. Beaupre, A., Choukroun, R., Guidouin, R., Garneau, R., Gerardin, H., and Cardou, A. Knee menisci. Correlation between microstructure and biomechanics. Clin Orthop Relat Res 72, 1986.
3. Krause, W.R., Pope, M.H., Johnson, R.J., and Wilder, D.G. Mechanical changes in the knee after meniscectomy. J Bone Joint Surg Am **58,** 599, 1976.
4. Walker, P.S., and Erkman, M.J. The role of the menisci in force transmission across the knee. Clin Orthop Relat Res 184, 1975.
5. Makris, E.A., Hadidi, P., and Athanasiou, K.A. The knee meniscus: structure-function, pathophysiology, current repair techniques, and prospects for regeneration. Biomaterials **32,** 7411, 2011.
6. Arnoczky, S.P., and Warren, R.F. Microvasculature of the human meniscus. Am J Sports Med **10,** 90, 1982.
7. Fauno, P., and Nielsen, A.B. Arthroscopic partial meniscectomy: a long-term follow-up. Arthroscopy **8,** 345, 1992.
8. Fairbank, T.J. Knee joint changes after meniscectomy. J Bone Joint Surg Br **30B,** 664, 1948.
9. Bullough, P.G., Munuera, L., Murphy, J., and Weinstein, A.M. The strength of the menisci of the knee as it relates to their fine structure. J Bone Joint Surg Br **52,** 564, 1970.
10. Petersen, W., and Tillmann, B. Collagenous fibril texture of the human knee joint menisci. Anat Embryol (Berl) **197,** 317, 1998.
11. Fox, A.J., Bedi, A., and Rodeo, S.A. The basic science of human knee menisci: structure, composition, and function. Sports Health **4,** 340, 2012.
12. Choi, N.H., Kim, T.H., Son, K.M., and Victoroff, B.N. Meniscal repair for radial tears of the midbody of the lateral meniscus. Am J Sports Med **38,** 2472, 2010.
13. Foad, A. Self-limited healing of a radial tear of the lateral meniscus. Knee Surg Sports Traumatol Arthrosc **20,** 933, 2012.
14. van Trommel, M.F., Simonian, P.T., Potter, H.G., and Wickiewicz, T.L. Arthroscopic meniscal repair with fibrin clot of complete radial tears of the lateral meniscus in the avascular zone. Arthroscopy **14,** 360, 1998.
15. Noyes, F.R., and Barber-Westin, S.D. Arthroscopic repair of meniscus tears extending into the avascular zone with or without anterior cruciate ligament reconstruction in patients 40 years of age and older. Arthroscopy **16,** 822, 2000.
16. Tao, S.S., and Beach, W.R. Use of a Caspari suture punch to repair a radial tear of the lateral meniscus. Arthroscopy **18,** 206, 2002.
17. Mauck, R.L., Baker, B.M., Nerurkar, N.L., Burdick, J.A., Li, W.J., Tuan, R.S., and Elliott, D.M. Engineering on the straight and narrow: the mechanics of nanofibrous assemblies for fiber-reinforced tissue regeneration. Tissue Eng Part B Rev **15,** 171, 2009.
18. Li, W.J., Mauck, R.L., Cooper, J.A., Yuan, X., and Tuan, R.S. Engineering controllable anisotropy in electrospun biodegradable nanofibrous scaffolds for musculoskeletal tissue engineering. J Biomech **40,** 1686, 2007.
19. Janjanin, S., Li, W.J., Morgan, M.T., Shanti, R.M., and Tuan, R.S. Mold-shaped, nanofiber scaffold-based cartilage engineering using human mesenchymal stem cells and bioreactor. J Surg Res **149,** 47, 2008.
20. Nerurkar, N.L., Baker, B.M., Sen, S., Wible, E.E., Elliott, D.M., and Mauck, R.L. Nanofibrous biologic laminates replicate the form and function of the annulus fibrosus. Nat Mater **8,** 986, 2009.
21. Ionescu, L.C., and Mauck, R.L. Porosity and cell preseeding influence electrospun scaffold maturation and meniscus integration in vitro. Tissue Eng Part A **19,** 538, 2013.
22. Henning, C.E., Yearout, K.M., Vequist, S.W., Stallbaumer, R.J., and Decker, K.A. Use of the fascia sheath coverage and exogenous fibrin clot in the treatment of complex meniscal tears. Am J Sports Med **19,** 626, 1991.
23. Pabbruwe, M.B., Kafienah, W., Tarlton, J.F., Mistry, S., Fox, D.J., and Hollander, A.P. Repair of meniscal cartilage white zone tears using a stem cell/collagen-scaffold implant. Biomaterials **31,** 2583, 2010.
24. Bhargava, M.M., Hidaka, C., Hannafin, J.A., Doty, S., and Warren, R.F. Effects of hepatocyte growth factor and platelet-derived growth factor on the repair of meniscal defects in vitro. In vitro Cell Dev Biol Anim **41,** 305, 2005.
25. Steinert, A.F., Palmer, G.D., Capito, R., Hofstaetter, J.G., Pilapil, C., Ghivizzani, S.C., Spector, M., and Evans, C.H. Genetically enhanced engineering of meniscus tissue using *ex vivo* delivery of transforming growth factor-beta 1 complementary deoxyribonucleic acid. Tissue Eng **13,** 2227, 2007.
26. Kobayashi, K., Fujimoto, E., Deie, M., Sumen, Y., Ikuta, Y., and Ochi, M. Regional differences in the healing potential of the meniscus-an organ culture model to eliminate the influence of microvasculature and the synovium. Knee **11,** 271, 2004.
27. Hennerbichler, A., Moutos, F.T., Hennerbichler, D., Weinberg, J.B., and Guilak, F. Repair response of the inner and outer regions of the porcine meniscus in vitro. Am J Sports Med **35,** 754, 2007.

28. McNulty, A.L., Moutos, F.T., Weinberg, J.B., and Guilak, F. Enhanced integrative repair of the porcine meniscus in vitro by inhibition of interleukin-1 or tumor necrosis factor alpha. Arthritis Rheum **56,** 3033, 2007.
29. Baker, B.M., Nathan, A.S., Huffman, G.R., and Mauck, R.L. Tissue engineering with meniscus cells derived from surgical debris. Osteoarthritis Cartilage **17,** 336, 2009.
30. Mauck, R.L., Martinez-Diaz, G.J., Yuan, X., and Tuan, R.S. Regional multilineage differentiation potential of meniscal fibrochondrocytes: implications for meniscus repair. Anat Rec (Hoboken) **290,** 48, 2007.
31. Magee, T., Shapiro, M., and Williams, D. MR accuracy and arthroscopic incidence of meniscal radial tears. Skeletal Radiol **31,** 686, 2002.
32. Chevrier, A., Nelea, M., Hurtig, M.B., Hoemann, C.D., and Buschmann, M.D. Meniscus structure in human, sheep, and rabbit for animal models of meniscus repair. J Orthop Res **27,** 1197, 2009.
33. Li, W.J., Cooper, J.A., Jr., Mauck, R.L., and Tuan, R.S. Fabrication and characterization of six electrospun poly(alpha-hydroxy ester)-based fibrous scaffolds for tissue engineering applications. Acta Biomater **2,** 377, 2006.
34. Fisher, M.B., Henning, E.A., Soegaard, N., Esterhai, J.L., and Mauck, R.L. Organized nanofibrous scaffolds that mimic the macroscopic and microscopic architecture of the knee meniscus. Acta Biomater **9,** 4496, 2013.
35. Fithian, D.C., Kelly, M.A., and Mow, V.C. Material properties and structure-function relationships in the menisci. Clin Orthop Relat Res 19, 1990.
36. Proctor, C.S., Schmidt, M.B., Whipple, R.R., Kelly, M.A., and Mow, V.C. Material properties of the normal medial bovine meniscus. J Orthop Res **7,** 771, 1989.
37. Moriguchi, Y., Tateishi, K., Ando, W., Shimomura, K., Yonetani, Y., Tanaka, Y., Kita, K., Hart, D.A., Gobbi, A., Shino, K., Yoshikawa, H., and Nakamura, N. Repair of meniscal lesions using a scaffold-free tissue-engineered construct derived from allogenic synovial MSCs in a miniature swine model. Biomaterials **34,** 2185, 2013.
38. Nakagawa, Y., Muneta, T., Kondo, S., Mizuno, M., Takakuda, K., Ichinose, S., Tabuchi, T., Koga, H., Tsuji, K., and Sekiya, I. Synovial mesenchymal stem cells promote healing after meniscal repair in microminipigs. Osteoarthritis Cartilage pii: S1063-4584(15)00050-3, 2015. doi: 10.1016/j.joca.2015.02.008.
39. Vargas, F., Vives-Pi, M., Somoza, N., Armengol, P., Alcalde, L., Marti, M., Costa, M., Serradell, L., Dominguez, O., Fernandez-Llamazares, J., Julian, J.F., Sanmarti, A., and Pujol-Borrell, R. Endotoxin contamination may be responsible for the unexplained failure of human pancreatic islet transplantation. Transplantation **65,** 722, 1998.
40. Jahr, H., Pfeiffer, G., Hering, B.J., Federlin, K., and Bretzel, R.G. Endotoxin-mediated activation of cytokine production in human PBMCs by collagenase and Ficoll. J Mol Med (Berl) **77,** 118, 1999.

Address correspondence to:
Rocky S. Tuan, PhD
Center for Cellular and Molecular Engineering
Department of Orthopaedic Surgery
University of Pittsburgh School of Medicine
450 Technology Drive, Suite 221
Pittsburgh, PA 15219-3143

E-mail: rst13@pitt.edu

Received: September 17, 2014
Accepted: March 25, 2015
Online Publication Date: May 4, 2015